Journal of Computational Physics 228 (2009) 8187–8202

Contents lists available at ScienceDirect

Journal of Computational Physics

journal homepage: www.elsevier.com/locate/jcp

A roe-average algorithm for a granular-gas model with non-conservative terms

Hemant Kamath [1,2], Xiaoju Du [*,2]

M.C.I., Faculty of Engineering, Alsion 2, University of Southern Denmark, DK-6400 Sønderborg, Denmark

ARTICLE INFO

Article history:
Received 19 February 2009
Received in revised form 2 August 2009
Accepted 11 August 2009
Available online 18 August 2009

Keywords:
Granular gases
Compressible flows
Shock waves

ABSTRACT

A Roe-average algorithm has been derived for a granular-gas model, proposed by Goldshtein and Shapiro [Goldshtein, Shapiro, Mechanics of collisional motion of granular materials: Part 1. General hydrodynamic equations, J. Fluid Mech. 282 (1995) 75–114], which contains non-conservative terms in the Euler-like hyperbolic governing equations apart from sink terms, which arise from inelastic collision of granules and are present only in the energy equation. The non-conservative terms introduce non-isentropic effects in acoustic-wave propagation within granular media and they also contribute to the Rankine–Hugoniot relations across a discontinuity. A Roe-average algorithm, based on the same granular-gas model, was derived in the literature [V. Kamenetsky, A. Goldshtein, M. Shapiro, D. Degani, Evolution of a shock wave in a granular gas, Phys. Fluids, 12 (2000) 3036–3049] which then required the implementation of a shock-fitting technique at a discontinuity. In the present work, Roe-averaged variables have been obtained from the Rankine–Hugoniot jump relations and the non-conservative terms have been incorporated in the numerical flux formula consistent with upwind principles associated with the granular speed of sound. Results for unsteady one-dimensional granular flows, colliding with a wall, demonstrate the capability of the proposed algorithm to capture strong shocks in addition to flow features not found in molecular gases, such as a fluidized region downstream of the shock and a compacted solid-block region adjacent to the wall.

1. Introduction

Flows of granular materials are encountered in many industrial-applications which store, transport or mix non-cohesive solid particles including agriculture, mining, chemical, pharmaceutical and food processing. To facilitate transport of a bed of solid particles, vibrations of a certain amplitude and frequency are often imparted to the conveyor unit to introduce fluidization within the medium. Granular media can be difficult to handle, resulting in inefficiency and delays in many process industries. The bulk motion of granules can be broadly subdivided into slow and fast flow regimes. In the slow flow regime, there is constant contact among particles during their motion, which is controlled by interparticle Coulomb-frictional forces. In contrast, the rapid flow regime involves freely moving particles which interact by fast-impact collisions. In such a case, inter-particle transfer of momentum and kinetic energy take place during collisions and the effective transport properties are governed by the nature of these collisions.

* Corresponding author.
E-mail address: duxju@hotmail.com (X. Du).
[1] From 08-06-1958 to 30-06-2006.
[2] Both authors contributed equally to this article.

0021-9991/$ - see front matter © 2009 Elsevier Inc. All rights reserved.
doi:10.1016/j.jcp.2009.08.005

Rapid granular flows, interacting through inelastic collisions, have been the subject of many experimental, theoretical and numerical investigations which have been reviewed in [2,7] among others. Particle impacts are accompanied by kinetic energy losses, associated with surface roughness and inelastic collisions, and a constant or periodic input of mechanical energy is required to sustain the collisional motion of moving granular media. The sources of mechanical energy could be pneumatic pressure, externally-induced vibrations, gravity or other applied body forces involving electric or magnetic fields, among others. Gravity force, which causes rapid shear flow of granular material down inclined surfaces, could also act as a source of energy in one-dimensional shearless granular flows such as those induced by a vibrofluidized mechanism. The hydrodynamic equations for modelling shear-induced rapid flows are similar to the Navier–Stokes equations in possessing viscosity and thermal conductivity terms [8,9,12,13]. However, in one-dimensional shearless granular flows, driven by some external source, the effects of viscosity and thermal conductivity are unimportant. Also, under moderate accelerations of the vibrating bed, experimental evidence of shock-wave propagation was presented in [4], following a derivation of compressible hydrodynamic equations for rigid particles of arbitrary inelasticity and roughness in [3] based on the Chapman–Enskog solution to the Boltzmann equation. A comprehensive study also included [5] an analytical solution of shock-wave propagation, based on the derived Euler-like hydrodynamic equations, for asymptotically large time when the solution becomes self-similar. Furthermore, the expansion wave problem was analysed in [6] and an analytical solution could be obtained in the dilute granular-gas approximation. This was followed by a computational study of shock-wave propagation in a granular gas in [10], based on Roe's approximate Riemann solver which was derived for the associated hydrodynamic equations.

The present work was necessitated by derivation of the Roe-averaged state [10] of the hyperbolic system of mass, momentum and energy equations for a granular gas re-derived in [3]. Firstly, the Roe-average state has been derived properly in this paper. Secondly, the energy equation now contains two types of sink terms due to inelastic collisions of granules. One of these terms, which is proportional to the divergence of velocity, cannot be cast in a divergence form, required for the application of many numerical schemes for hyperbolic conservation laws. This non-conservative term influences [3] the speed of sound, which is the speed of propagation of infinitesimal disturbances in a granular gas. Not only is acoustic-wave propagation a non-isentropic process, due to this, but the term also enters [3] the Rankine–Hugoniot jump relations across a discontinuity. In [10], the non-conservative term was arbitrarily and alternately assigned to either the positive or negative contributions to Roe's interface-flux formula for one-dimensional unsteady computations. Such a treatment may not work for multi-dimensional computations and cannot be directly extended to unstructured grids. In the present work, the non-conservative term is uniformly incorporated into the numerical flux formula to be consistent with upwind principles associated with the granular speed of sound. Non-conservative terms often arise in governing equations encountered in turbulence modelling and the present work may be of relevance in other applications as well.

The paper has been organized in the following manner: the next section briefly presents the governing equations for unsteady one-dimensional compressible granular flows. Sections 3 and 4 deal with Roe's algorithm for the hyperbolic governing equations with non-conservative terms and the MUSCL-Hancock time-integration procedure, respectively. Results for some test cases are presented in Section 5 to demonstrate the shock-capturing capability of the proposed algorithm for granular-gas flows, in addition to resolving flow features not found in molecular gases. Section 6 contains concluding remarks.

2. Governing equations for compressible granular flows

The unsteady, one-dimensional Euler-like governing equations for motion of a granular gas can be expressed [3,10] as follows:

$$\frac{\partial U}{\partial t}+\frac{\partial F(U)}{\partial x}+B(U)\frac{\partial U}{\partial x}=S(U) \tag{1}$$

where the matrix B contains the non-conservative terms in the energy equation arising from inelastic collisions. U is the vector of dependent variables, F is the flux vector and S is the source vector, containing gravity contributions in the momentum and energy equations, apart from a sink term in the energy equation also due to inelastic collisions. These terms, in expanded form, are:

$$U=\begin{bmatrix}\rho\\ \rho u\\ E\end{bmatrix}F=\begin{bmatrix}\rho u\\ \rho u^2+P\\ u(E+P)\end{bmatrix}B=\begin{bmatrix}0 & 0 & 0\\ 0 & 0 & 0\\ \frac{\mathcal{P}}{\rho}u & -\frac{\mathcal{P}}{\rho} & 0\end{bmatrix}S=\begin{bmatrix}0\\ \rho g\\ \rho u g+I\end{bmatrix} \tag{2}$$

where ρ is the granular-gas density, u is the velocity, P is the pressure and E is the total granular energy per unit volume, $E=\rho\epsilon+\rho u^2/2$ with ϵ being the internal energy per unit mass. The terms I and $\mathcal{P}$, in the energy equation, due to inelastic collisions, are [10]:

$$I=C_0\frac{\sigma^2}{m}\rho^2\epsilon^{3/2}g(\nu) \tag{3}$$

$$\mathcal{P}=\rho\epsilon\alpha_t[C_1+2C_2(1+e)\nu g(\nu)] \tag{4}$$

$$g(\nu)=[1-(\nu/\nu_M)^{4\nu_M/3}]^{-1} \tag{5}$$

where σ is the diameter of a particle with mass m and density ρ_p, e is the restitution coefficient and $v \equiv \rho/\rho_p$, the solid fraction, is the volume of solids per unit volume of the granular gas, with v_M being its maximum attainable value for a prescribed packing configuration. For closest random-packing of spheres $v_M = 0.64$ and it varies from $\pi/6$, for simple cubic, to 0.74 for face-centered cubic packing. The parameters C_0, C_1, C_2 and α_t are analytical functions of e and a roughness parameter, β, as obtained in [3] and are defined in Appendix B. The equilibrium radial distribution function, $g(v)$, as defined in (5), is more accurate [5] near the maximum-packing limit (even though it is singular at v_M) as compared to the dilute-gas limit which yields the following [10] equation of state for a granular gas:

$$P = \rho\epsilon G(v) \text{ with } G(v) \equiv \alpha_t[1 + 2(1+e)vg(v)] \tag{6}$$

Shock waves are commonly encountered in granular-gas flows since the speed of sound is extremely low compared to that of molecular gases. Furthermore, unlike in molecular gases, the kinetic energy of random motion, which is often referred to as granular temperature, continually decreases as a result of inelastic particle collisions. Even for a simple flow involving preservation of uniform conditions, the sink term in the energy equation, due to inelastic collisions, causes diminishing of pressure with time, for non-zero granular temperature, and consequently also for the speed of sound, whereas constancy is maintained only for density and velocity variables. It was shown in [5] that this volumetric energy-dissipation term, I (3), leads to interesting consequences downstream of a shock due to increased particle collisions with an attendant increase in granular-gas density. In particular, for the classical problem of shock wave generated by a moving piston, the distribution of gas-dynamic variables between the shock and the piston is nonuniform. On the piston, a solid block comprising densely-packed granules is formed after some time and this continuously-growing layer is separated from the shock front by a non-uniform fluidized region. In the latter region, the granular kinetic energy is constantly diminishing, due to an increase in inelastic non-conservative collisions downstream of the shock to the start of the solid block.

The governing Eq. (1) are not valid within the solid block due to the singularity of $g(v)$ in (5) as $v \to v_M$ which results in pressure and speed of sound approaching infinity, a manifestation of rapidly decreasing compressibility of the medium. To enable computations to be performed uniformly all the way to the piston, a granular-flow model was proposed in [10], which switches off the energy-dissipation terms when the solids fraction, v, exceeds a cut-off value, v_c, that is less than the maximum permissible value, v_M. It was shown in [10] that, if v_c was chosen sufficiently close to v_M then numerical results, using this granular-flow model, agree with the limiting analytical solution, derived in [5] for the fluidized region, valid after sufficiently longtime-propagation of the shock. Furthermore, a density-dependent restitution coefficient was introduced in [10] to account for the elastic nature of granular collisions, when their kinetic energy approaches zero, based on a cut-off criterion:

$$e_c = \begin{cases} e & \text{for} \quad v < v_c \\ 1 & \text{for} \quad v \geqslant v_c \end{cases} \tag{7}$$

A similar limiting condition was imposed on β, resulting in I and $\mathcal{P}$ being set to zero when the granular gas is compressed beyond the cut-off limit, v_c, so that it then reduces to a conservative gas possessing a very large speed of sound within the solid block. Such a criterion was not imposed in [16] and hence the computations reported could be carried out only until the start of formation of solid block at the wall. Furthermore, the granular-flow model of [16] did not contain any non-conservative terms in the governing equations which ensured that acoustic-wave propagation remained an isentropic process as in a molecular gas. However, this model did contain source terms similar to I in (2) apart from gravitational-source terms in the momentum and energy equations, as in the present work. These gravitational-source terms also need to be set to zero within the solid block to ensure that the governing equations reduce to a form appropriate for a conservative gas.

3. Roe's algorithm for the non-conservative governing equations

For a hyperbolic system of conservation laws, Roe's algorithm [14] involves solution of the homogeneous linearized governing equations:

$$U_t + \widehat{A}U_x + \widehat{B}U_x = 0 \tag{8}$$

where the matrices $\widehat{A}$ and $\widehat{B}$ refer to $A \equiv dF/dU$, the Jacobian matrix of the flux vector, and the matrix B in (2), evaluated at the so-called Roe-averaged state, $\widehat{U} \equiv \widehat{U}(U_L, U_R)$, which is a function of the corresponding left and right states at an interface of a computational cell. The matrix A has a complete set of eigenvectors but B does not in the present case. Furthermore, the eigenvalues of $A + B$ are:

$$\lambda_1 = u - c; \lambda_2 = u; \lambda_3 = u + c \tag{9}$$

where c is the speed of sound in a granular gas:

$$c = [(E - \rho u^2/2)G_\rho + \mathcal{H}G - Gu^2/2]^{1/2} \text{ with } \mathcal{H} \equiv (E + P - \mathcal{P})/\rho \tag{10}$$

This is the speed of infinitesimal disturbances, which do not propagate isentropically, and can be derived [3] by casting the governing Eq. (1) in characteristic form. In contrast, the isentropic propagation of small-amplitude acoustic waves in a molecular gas permits the algebraic expression for the speed of sound to be directly derived from the equation of state.

The term $\mathcal{P}$, which arises due to inelastic granular collisions, is not only responsible for non-isentropic propagation of infinitesimal disturbances but it also contributes to the Rankine–Hugoniot jump relations, across an isolated discontinuity of arbitrary strength, which is involved in the determination of the Roe-average state (See Appendix A). The expression for the speed of sound in (10) is appropriate for the prescription of Roe-averaged variables but, using (4), (6), it can be recast in the following form:

$$c^2 = \Gamma(\rho)\frac{P}{\rho} \text{ with } \Gamma(\rho) \equiv \rho\frac{G_\rho}{G} + 1 + G - \alpha_t[C_1 + 2C_2(1+e)\nu g(\nu)] \tag{11}$$

in which the functional dependence of Γ only on ρ is revealed. It should be noted that in this expression for the sound speed, the terms containing C_1 and C_2 are due to the B matrix in (1) that introduce non-isentropic effects caused by inelastic collisions. The matrix of right eigenvectors, R, of $A + B$ is:

$$R = \begin{bmatrix} 1 & -2 & 1 \\ u-c & -2u & u+c \\ \mathcal{H}-uc & 2[c^2/G - \mathcal{H}] & \mathcal{H}+uc \end{bmatrix} \tag{12}$$

and its inverse is:

$$R^{-1} = \frac{1}{2c^2}\begin{bmatrix} (E-\rho u^2/2)G_\rho + Gu^2/2 + uc & -uG - c & G \\ (E-\rho u^2/2)G_\rho + Gu^2/2 - c^2 & -uG & G \\ (E-\rho u^2/2)G_\rho + Gu^2/2 - uc & -uG + c & G \end{bmatrix} \tag{13}$$

Jump conditions for the non-conservative granular-gas model are obtained by Goldshtein and Shapiro [4], which coincide with the Rankine–Hugoniot conditions and there is no contribution of the energy dissipation term to the energy jump condition. In the following, a jump condition for the present granular-gas model with a velocity divergent sink term is derived. We assume that a discontinuity propagates with velocity $s(x,t)$ in a sufficiently small neighborhood N, where function $U(x,t)$ satisfies equation in the following form:

$$\frac{\partial U}{\partial t} + \frac{\partial F(U)}{\partial x} + B(U)\frac{\partial U}{\partial x} = 0 \tag{14}$$

We also assume that weak solution $U(x,t)$ is differentiable and bounded in this neighborhood. By introducing a test function $\Phi(x,t)$ with support in N [21], a more general form of the jump condition could be obtained as:

$$s(U_R - U_L) = F(U_R) - F(U_L) + \int_{U_L}^{U_R} B(U)dU \tag{15}$$

where $s = x'(t)$. The additional term $\int B(U)$ normally is not included in the Rankine–Hugoniot condition for the conservation of U across the discontinuities. It should be noticed that the velocity divergent term $B(U)$ is a bounded function in N [20]:

$$\int_{U_R}^{U_L} B(U)dU \approx \frac{1}{2}(B(U_L) + B(U_R))(U_R - U_L) \tag{16}$$

Since this bounded sink term still obeys the Rankine–Hugoniot jump condition, which holds across the discontinuities with velocity s, it can be obtained as follows:

$$s(U_R - U_L) = F(U_R) - F(U_L) + \frac{1}{2}(B(U_L) + B(U_R))(U_R - U_L) \tag{17}$$

It can be inferred from (2) that the arithmetic average of the matrix representing non-conservative terms, B, will contribute only to the energy jump condition whereas the mass and momentum jump relations have a form similar to that for a molecular gas. This contribution will vanish only when $\mathcal{P} \equiv 0$ for the case $e = 1 = |\beta|$, which would correspond to the conservative-gas limit. The Roe-averaged state is determined by requiring s to be an eigenvalue of the matrix combination $\widehat{A} + \widehat{B}$, appearing in the linearized system of governing equations (8), for an isolated discontinuity of arbitrary strength, which yields the condition:

$$(\widehat{A} + \widehat{B})(U_R - U_L) = F(U_R) - F(U_L) + \frac{1}{2}(B(U_L) + B(U_R))(U_R - U_L) \tag{18}$$

This can be decomposed further into two separate conditions by noting that terms involving $\mathcal{P}$ must balance out on both sides of the above equation:

$$\widehat{A}(U_R - U_L) = F(U_R) - F(U_L) \tag{19}$$

$$\widehat{B}(U_R - U_L) = \frac{1}{2}(B(U_L) + B(U_R))(U_R - U_L) \tag{20}$$

The Jacobian matrix of the flux vector $A \equiv dF/dU$, evaluated at the Roe-averaged state, can be determined as in [10]:

$$\widehat{A} = \begin{bmatrix} 0 & 1 & 0 \\ \hat{\rho}\epsilon\widehat{G}_\rho + \widehat{G}\hat{u}^2/2 - \hat{u}^2 & (2-\widehat{G})\hat{u} & \widehat{G} \\ \hat{\rho}\epsilon\hat{u}\widehat{G}_\rho + \widehat{G}\hat{u}^3/2 - \widehat{H}\hat{u}/\hat{\rho} & -\hat{u}^2\widehat{G} + \widehat{H}/\hat{\rho} & (1+\widehat{G})\hat{u} \end{bmatrix} \tag{21}$$

where $H \equiv E + P$ is the total enthalpy per unit volume of the granular gas. The Roe-averaged matrix $\widehat{A}$ contains six variables, $\hat{\rho}, \hat{u}, \widehat{H}, \hat{\rho}\epsilon, \widehat{G}$ and $\widehat{G}_\rho$, which need to be determined from (19). Also, as inferred from (2), the Roe-averaged matrix $\widehat{B}$ contains only one variable, $\widehat{\mathcal{P}}$, which must be obtained from (20) assuming that $\hat{\rho}$ and $\hat{u}$ have already been prescribed. It should be noted that ρ could have been absorbed in H by introducing an alternative variable which would represent the total enthalpy per unit mass of the granular gas. Similarly ρ could have also been combined with $\mathcal{P}$, which then eliminates density from the Roe-averaged variables that need to be prescribed for a non-iterative solution procedure of the under-determined system of algebraic equations resulting from the constraints (19) and (20). Even for a molecular gas satisfying the perfect-gas law, where the constraint on the Roe-averaged matrix completely determines the corresponding variables (which are averages of velocity and total enthalpy per unit mass), it is advantageous to introduce a density average to simplify the form of the linearized characteristic variable that appears in the expression for the numerical flux formula.

Roe-averages for density, velocity and total enthalpy per unit volume can be conveniently defined similar to that for a molecular gas satisfying an arbitrary gas law [11]:

$$\hat{\rho} = \sqrt{\rho_L\rho_R}\hat{u} = [u_L\sqrt{\rho_L} + u_R\sqrt{\rho_R}]/[\sqrt{\rho_L} + \sqrt{\rho_R}] \tag{22}$$

$$\widehat{H} = [H_L\sqrt{\rho_R} + H_R\sqrt{\rho_L}]/[\sqrt{\rho_L} + \sqrt{\rho_R}] \tag{23}$$

It should be noted that the density weights are switched in (23), since H here is not the total enthalpy per unit mass as is conventionally defined [11], but the two formulae are mathematically equivalent. The constraint (20) can now be directly solved for $\widehat{\mathcal{P}}$ (See Appendix A for derivation):

$$\widehat{\mathcal{P}} = \frac{1}{2}\left[\mathcal{P}_L\frac{\rho_R}{\rho_L} + \mathcal{P}_R\frac{\rho_L}{\rho_R}\right] \tag{24}$$

It is easy to see that $\widehat{B} \neq (B(U_L) + B(U_R))/2$ in general. With the definitions (22) and (23), the constraint (19) reduces to (please refer to Appendix A for detailed derivation):

$$\hat{\rho}\epsilon\widehat{G}_\rho(\rho_R - \rho_L) + \widehat{G}(P_R/G_R - P_L/G_L) = P_R - P_L \tag{25}$$

which is one equation for the three averages $\hat{\rho}\epsilon, \widehat{G}$ and $\widehat{G}_\rho$ that leads to non-unique prescriptions. Noting that $E - \rho u^2/2 \equiv \rho\epsilon$, the following averages can be prescribed as in [10]:

$$\hat{\rho}\epsilon = [(\rho\epsilon)_L\sqrt{\rho_R} + (\rho\epsilon)_R\sqrt{\rho_L}]/[\sqrt{\rho_L} + \sqrt{\rho_R}] \tag{26}$$

$$\widehat{G}_\rho = \begin{cases} dG/d\rho & \text{for} \quad \rho_R = \rho_L \\ [G(\rho_R) - G(\rho_L)]/[\rho_R - \rho_L] & \text{for} \quad \rho_R \neq \rho_L \end{cases} \tag{27}$$

The prescription for $\hat{\rho}\epsilon$ with the switched density weights in (26) is mathematically equivalent to that for $\hat{\epsilon}$, proposed for a real gas in [11] with ρe and e being internal energies defined on a unit volume and unit-mass basis, respectively. Now, (25) can be solved for the only average that remains unspecified:

$$\widehat{G} = [G_L\sqrt{\rho_L} + G_R\sqrt{\rho_R}]/[\sqrt{\rho_L} + \sqrt{\rho_R}] \tag{28}$$

In [10], $\widehat{\mathcal{P}}$ has been specified as the arithmetic averages of left and right values, which is different from (24), and furthermore $\widehat{G}$ has not been prescribed at all. It should be noted that $\widehat{G}$ cannot be taken as $G(\hat{\rho})$ since such a prescription will not satisfy the constraint (25) in general. However, specification of the Roe-averaged state in [10] will not significantly affect the accuracy of the results presented therein since a shock-fitting technique was employed at a discontinuity where the largest error is expected to occur. In the present research, the derivation of the Roe-averaged state enables any gas-dynamic discontinuity to be captured by construction since the resulting algorithm will be consistent with the associated Rankine–Hugoniot jump relations; detailed discussion can be found in Appendix A.

The interface flux $F_I(U_L, U_R)$ can be obtained from (18) and (20) by decomposing $\widehat{A} + \widehat{B}$ into positive and negative contributions, at an interface of a computational cell, as follows:

$$\widehat{R}\widehat{\Lambda}^+\widehat{R}^{-1}(U_R - U_L) = F(U_R) - F_I(U_L, U_R) + \widehat{B}U_R \tag{29}$$

$$\widehat{R}\widehat{\Lambda}^-\widehat{R}^{-1}(U_R - U_L) = F_I(U_L, U_R) - F(U_L) - \widehat{B}U_L \tag{30}$$

where $\widehat{\Lambda}^\pm$ are diagonal matrices containing positive and negative eigenvalues, respectively. It should be noted that in (29) and (30) the term containing the non-hyperbolic $\widehat{B}$ matrix, which contributes only to the energy flux, has been resolved into left and right components and allocated to the corresponding flux terms. This treatment ensures the symmetry of the two expressions for the interface flux with an interchange of left and right states as is also the case for a molecular gas where the non-conservative term is absent. Solving (29) and (30) for $F_I(U_L, U_R)$ and averaging the two expressions yields Roe's flux formula suitable for algorithmic implementation:

$$F_I(U_L,U_R)=\frac{1}{2}[F(U_L)+F(U_R)+\widehat{B}(U_L+U_R)]-\frac{1}{2}(\widehat{R}|\widehat{\Lambda}|\widehat{R}^{-1})(U_R-U_L) \tag{31}$$

This formula reduces to $F(U_L)+\widehat{B}U_L$ for supersonic flow from left to right, based on a Mach number constructed using Roe-averaged variables, which is consistent with the upwind principles associated with the granular speed of sound for the linearized representation of the B matrix in the system of governing equations. In contrast, Roe's flux formula, presented in [10], alternately allocates the non-conservative term to either the positive or the negative components in (29) and (30) and the resulting formula is not suited for multi-dimensional computations, particularly with unstructured grids. The uniform treatment of the non-conservative term in (31) ensures straightforward extensions of this formula to higher dimensions, which is beyond the scope of the current work and can be developed in the future.

At steady state, the consistency requires balancing of flux and non-conservative term at an interface:

$$F^n_{j+1}-F^n_j+B^n_{j+1/2}\left(U^n_{j+1}-U^n_j\right)=0 \tag{32}$$

which can be split into two equations by introducing flux $F^n_{j+1/2}$:

$$F^n_{j+1}-F^n_{j+1/2}+\frac{1}{2}B^n_{j+1/2}\left(U^n_{j+1}-U^n_j\right)=0 \tag{33}$$

and

$$F^n_{j+1/2}-F^n_j+\frac{1}{2}B^n_{j+1/2}\left(U^n_{j+1}-U^n_j\right)=0 \tag{34}$$

The following expression is obtained by shifting the index of Eq. (33):

$$F^n_j-F^n_{j-1/2}+\frac{1}{2}B^n_{j-1/2}\left(U^n_j-U^n_{j-1}\right)=0 \tag{35}$$

We eliminate the term F^n_j by adding two Eqs. (34) and (35):

$$F^n_{j+1/2}-F^n_{j-1/2}+\frac{1}{2}B^n_{j+1/2}\left(U^n_{j+1}-U^n_j\right)+\frac{1}{2}B^n_{j-1/2}\left(U^n_j-U^n_{j-1}\right)=0 \tag{36}$$

Then the non-conservative term in the linearized equation will be specified as the arithmetic average of the values at two interfaces to ensure the consistent of the scheme.

4. MUSCL-Hancock time-integration procedure

In a finite-volume implementation of the two-step MUSCL-Hancock procedure [19], the gas-dynamic variables, averaged over the computational cell length, are advanced using a midpoint rule in time with a piecewise linear reconstruction in space. In the present research, source terms, due to gravity and inelastic collisions, contain gas-dynamic variables and these must be properly represented in both steps of the time-integration procedure. The very low speed of sound in granular flows results in Mach numbers ranging from nearly zero within the solid block to hypersonic in the uniform flow region upstream

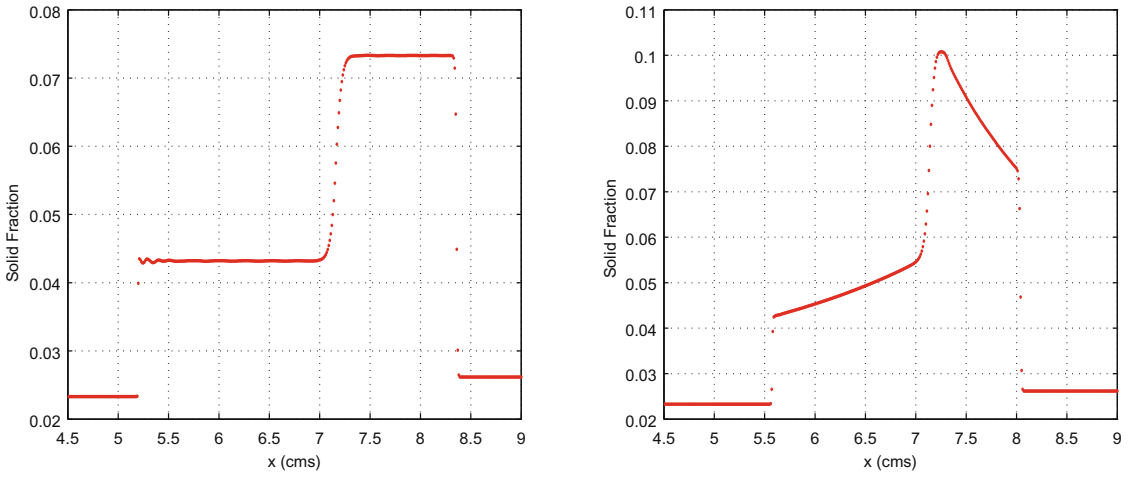

Fig. 1. The volume fraction of one-dimensional blast wave at time 5.48. Left: restitution coefficient $e=1$, right: $e=0.9$.

of the shock. An upwind formulation [1,15] of source terms, valid when Roe's algorithm is employed for the numerical fluxes, is incorporated in the MUSCL-Hancock procedure.

In the first step of this procedure, the primitive-variable vector $V = [v \equiv 1/\rho, u, p]^T$ for a computational cell j is advanced to half-time level based on a Taylor's series expansion:

$$V(x,t) = V_j^n + (x - x_j)(V_x)_j^n + (t - t^n)(V_t)_j^n \tag{37}$$

with $x_{j-1/2} < x < x_{j+1/2}$ and $t^n \leqslant t \leqslant t^{n+1/2}$, where $(V_t)_j^n \equiv (dV/dU)_j^n (U_t)_j^n$ and $(U_t)_j^n$ can be obtained from (1) as follows:

$$(U_t)_j^n = -\left[\frac{\left(F_{j+1/2}^n - F_{j-1/2}^n\right)}{\Delta x}\right] - \left[\frac{B_{j+1/2}^n}{2}\left(\frac{\left(U_{j+1}^n - U_j^n\right)}{\Delta x}\right)\right] - \left[\frac{B_{j-1/2}^n}{2}\left(\frac{\left(U_j^n - U_{j-1}^n\right)}{\Delta x}\right)\right] + S_j^n \tag{38}$$

The non-conservative term BU_x has been represented here as the arithmetic average of the values at the two interfaces, which is different from that proposed in [10] based on a cell-centered formulation. Furthermore, in the present research, the term S_j^n is prescribed by projecting the source-term vector onto the eigenvectors of the $A + B$ matrix at the two interfaces and accounting for the upwind and downwind contributions, respectively, at $(j - 1/2)$ and $(j + 1/2)$:

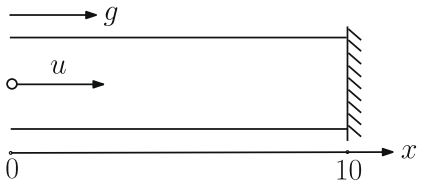

Fig. 2. Unsteady one-dimensional granular flows colliding with a wall.

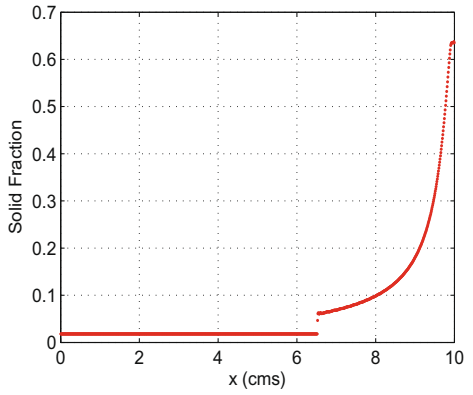

(a) *Volume fraction.*

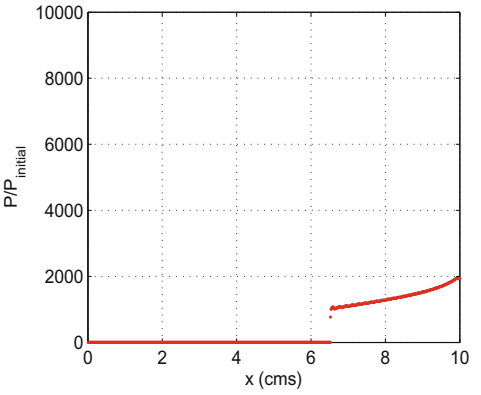

(b) *Ratio of pressure and initial value.*

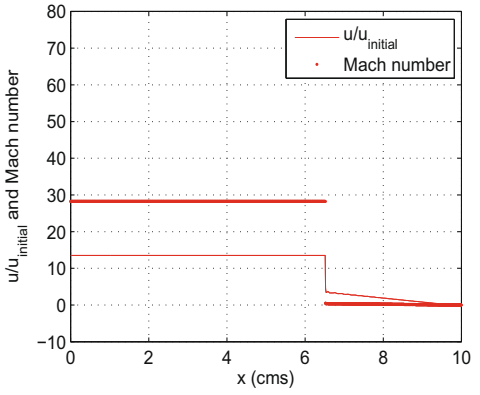

(c) *Ratio of velocity and its initial value and Mach number.*

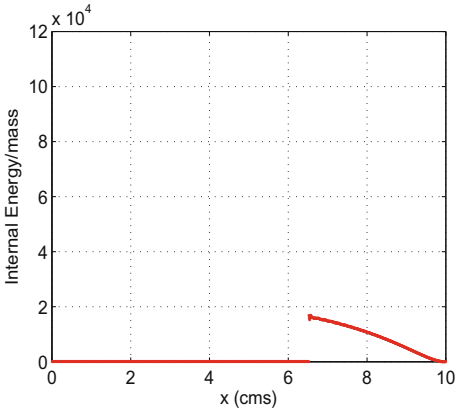

(d) *Internal energy per unit mass.*

Fig. 3. Case 1: inelastic and rough granular gas, accelerated under the action of gravity, hits a wall at rest (at right boundary) when the packed bed forms at time 0.23.

$$S_j^n \equiv \frac{1}{2}[I + |A+B|(A+B)^{-1}]_{j-1/2}^n S_{j-1/2}^n + \frac{1}{2}[I - |A+B|(A+B)^{-1}]_{j+1/2}^n S_{j+1/2}^n \tag{39}$$

It should be noted that all interface quantities in (38) and (39) are calculated using Roe-averaged variables. The limited gradients $(V_x)_j^n$ in (37) are obtained by first using a min-mod limiter [18] on the primitive variables $[v, u, p]^T$ and then differentiating the equation of state (6) to determine the limited gradient of the specific volume. This limiting procedure is more robust for hypersonic flows where the internal energy contribution to the total energy can be very small compared to the kinetic energy contribution.

The second-step of the MUSCL-Hancock procedure is the time-centered representation of (1) as follows:

$$\frac{\left(U_j^{n+1} - U_j^n\right)}{\Delta t} = (U_t)_j^{n+1/2} \tag{40}$$

where $(U_t)_j^{n+1/2}$ is obtained analogous to (38) by evaluating all variables at the half-time level, using (37) for the determination of interface and cell-centered values at $t = t^{n+1/2}$, including those appearing in the source terms of (39).

The boundary conditions are implemented by the ghost cell approach where all the primitive variables are calculated by linearly extrapolating the known quantities from the corresponding cells at inlet and outlet. And the boundary condition of the wall, is treated as a 'mirror' cell, with the same values of volume fraction and pressure as the interior cell, but with opposite velocities.

5. Results and discussion

In this section, we attempt to testify the reliability of the above Roe-averaged algorithm for solving the granular model with dissipation term. Some numerical experiments are performed and presented in the following.

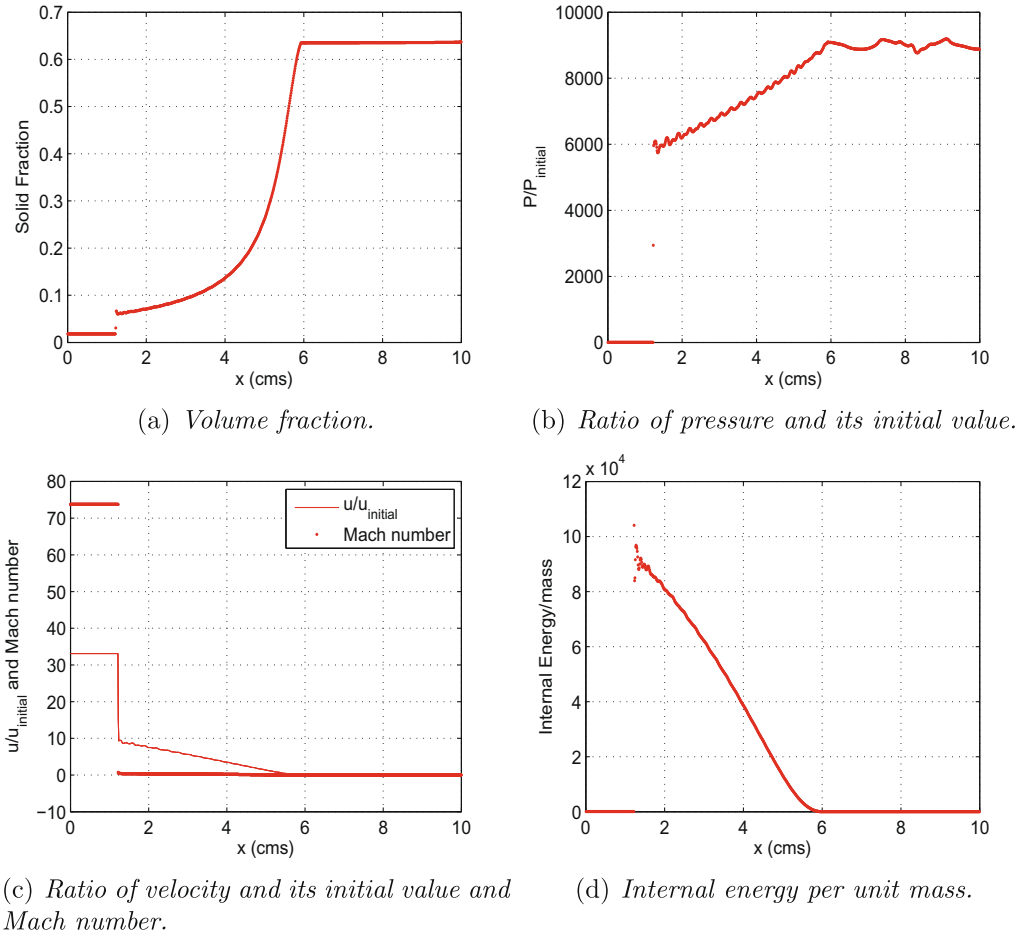

(a) *Volume fraction.* (b) *Ratio of pressure and its initial value.*

(c) *Ratio of velocity and its initial value and Mach number.* (d) *Internal energy per unit mass.*

Fig. 4. Case 1: inelastic and rough granular gas, accelerated under the action of gravity, hits a wall at rest (at right boundary) when the packed bed forms at time 0.59.

5.1. Tests of one-dimensional blast waves

We consider a Rimmen problem constructed by Serna and Marquina [17] to verify the Roe-average algorithm for a granular-flow model in this test case. The predicted results are computed with the non-divergent sink term $\mathcal{P} = 0$, coefficients $\alpha_t = 4/3$ and $C_0 = -\sqrt{\pi/2}\,\alpha_t^{3/2}(1 - e^2)$ to let the dissipation term I to be consistent with the Haff's cooling law in [17]. The initial left and right states are:

$$V_L = \begin{bmatrix} 1/\rho \\ u \\ P \end{bmatrix} = \begin{bmatrix} 1/44.5 \\ 0.698 \\ 3.528 \end{bmatrix} \tag{41}$$

and

$$V_R = \begin{bmatrix} 1/\rho \\ u \\ P \end{bmatrix} = \begin{bmatrix} 1/50 \\ 0 \\ 0.571 \end{bmatrix} \tag{42}$$

The total length is 10 cm with a grid of 1000 cells and the initial discontinuity is located in the middle. The Courant–Friedrichs–Lewy (CFL) is restricted under a constant which is expressed as $(|u| + c)_{max}\Delta t/\Delta x$ and the CFL number is equal to 0.8 in the blast wave case. The structure, consisted of shock, contact discontinuity and shock is predicted with restitution coefficients $e = 1$, where the dissipation term I vanishes and $e = 0.9$, where I is switched on. The numerical results in Fig. 1 behave well, compared with Serna and Marquina's [17] on the same mesh.

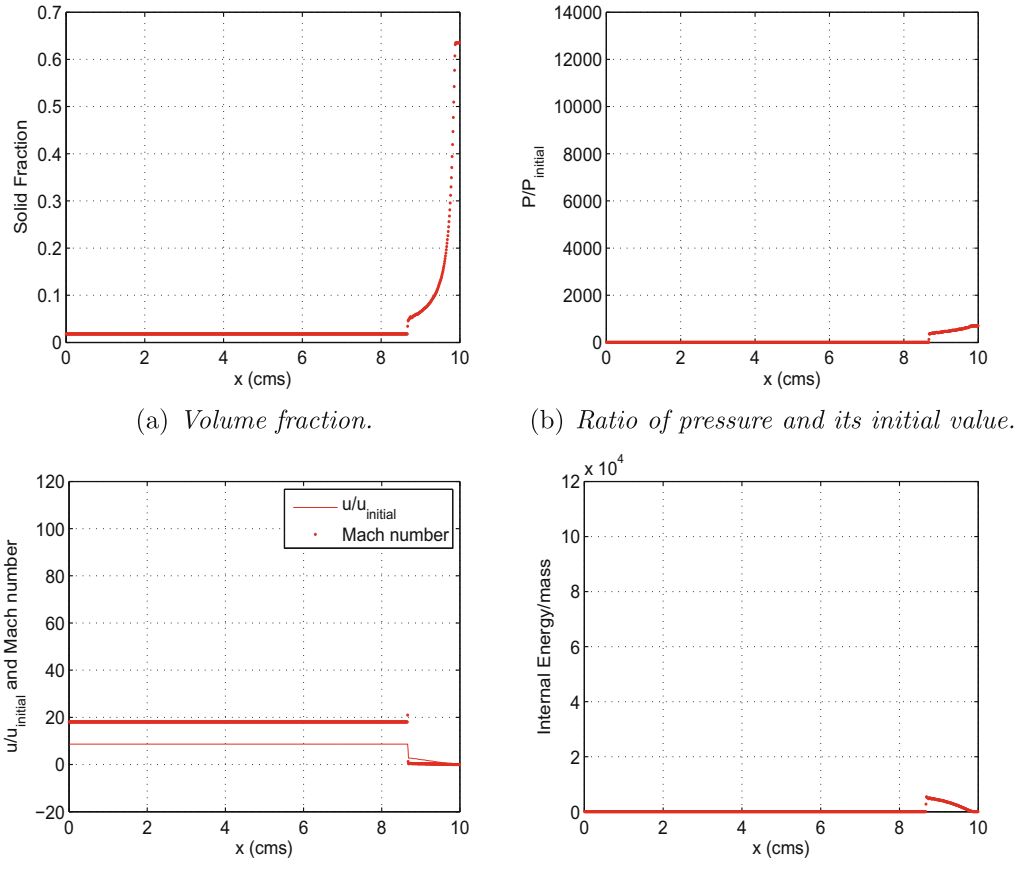

(a) *Volume fraction.* (b) *Ratio of pressure and its initial value.*

(c) *Ratio of velocity and its initial value and Mach number.* (d) *Internal energy per unit mass.*

Fig. 5. Case 2: inelastic and rough granular gas, accelerated under the action of gravity, hits a wall at rest (at right boundary) when the packed bed forms at time 0.14.

5.2. Tests of one-dimensional granular flows colliding with a wall

The capability of the above algorithm to capture strong shocks is now demonstrated by another two test cases which describe the behaviour of unsteady one-dimensional granular flows colliding with a wall under various physical situations. In Fig. 2, it shows the basic concept of particles, which have uniform diameter with $\sigma = 0.1$ moving randomly toward the wall under the influence of gravity accelerated in x direction (perpendicular to the wall). The finite length from the inlet to the wall is set to be 10 cm with a grid of 1000 cells for numerical experiments and the number of CFL criterion is equal to 0.5. In this section, we focus only on cases with an external energy source, provided by gravity, where the gravity acceleration $g = 9.8\ \mathrm{m/s^2}$, but without consideration of drag force. Initial values are derived from reference [16] with volume fraction $v = 0.018$ and speed of sound $c = 9\ \mathrm{m/s}$. And other values, calculated from the above quantities are $V = [1/\rho, u, P]^T = [1/34.37, 18, 1556.89]^T$ initially. The dissipation term will disappear when v_c is no less than 0.635 as the particles pack near the wall. The other parameters in the dissipation term and non-divergent term could be calculated with the equations given in Appendix B.

5.2.1. Test 1 without non-divergent term

In Case 1 (Figs. 3 and 4), the restitution coefficient $e = 0.97$, and roughness $\beta = 0.92849$. The loss of kinetic energy in the granular-gas approaches to zero when the absolute values of restitution e and roughness β are close to unity, corresponding to the conservative-gas limit. The contribution of the non-divergent sink term, $\mathcal{P}$, vanishes, reducing the complexity of this case both mathematically and physically. Fig. 4 indicates that there is a region at the wall where the density of granular gas is equal to ρ_{cut}, and the velocity vanishes where the particles are blocked. When the densely packed bed is formed, Mach numbers are small and the volumetric dissipation stops at the solid block. The values of internal energy per unit mass are not as large as in other regions because the contribution of total energy per unit volume is small. Some disturbances are observed in the pressure distribution, called pressure waves [10], at the packed bed.

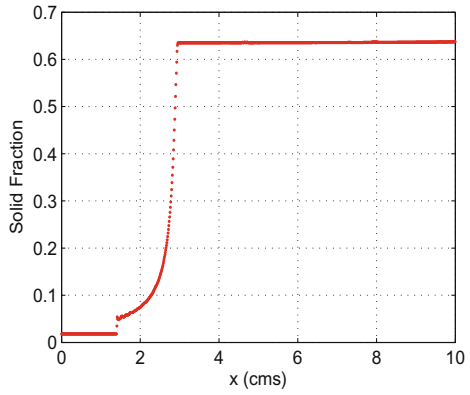

(a) *Volume fraction.*

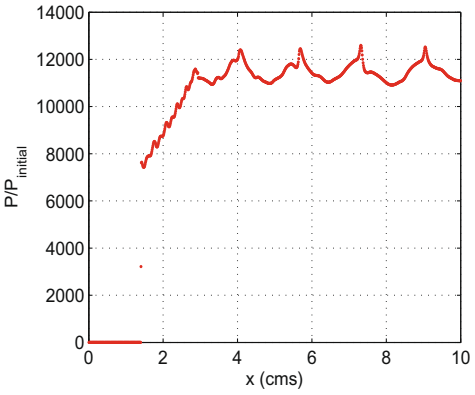

(b) *Ratio of pressure and its initial value.*

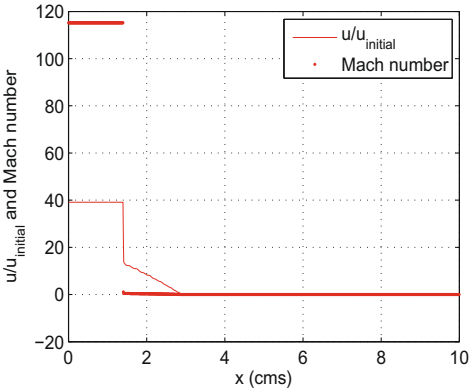

(c) *Ratio of velocity and its initial value and Mach number.*

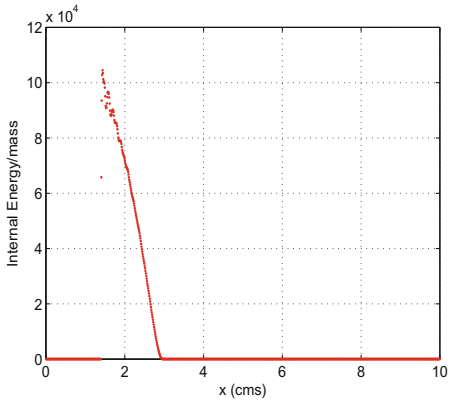

(d) *Internal energy per unit mass.*

Fig. 6. Case 2: inelastic and rough granular gas, accelerated under the action of gravity, hits a wall at rest (at right boundary) when the packed bed forms at time 0.7.

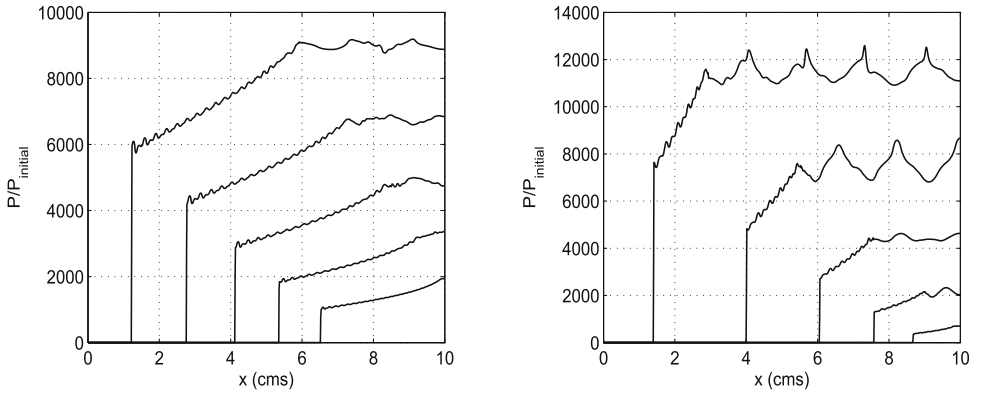

(a) *Case 1 at times* 0.59, 0.50, 0.41, 0.32 *and* 0.23.

(b) *Case 2 at times* 0.70, 0.56, 0.42, 0.28 *and* 0.14.

Fig. 7. Pressure time history from 0 to 10 cm.

The average value of pressure at the fluidized region increases and the speed of sound decreases as the shock advances. The level of internal energy tends to zero because more kinetic energy is supplied to the particle flow, to compensate for the energy dissipation due to inelastic collisions, which also leads the decreasing of pressure. However, density of particles keeps its initial values at the upstream of shock front. The results in Fig. 3 coincides well with those simulated by Serna and Marquina [16]. The cut-off point, v_{cut}, is not considered in their model and neither is the non-divergent sink term, $\mathcal{P}$, whereas this term will play a role during the computation in the following case.

5.2.2. Test 2 with non-divergent term

The non-divergent sink term is switched on in Case 2 (Figs. 5 and 6). The parameters of restitution and roughness are $e = 0.9$ and $\beta = -0.5566$, and both dissipation and gravity terms are active. In contrast to the ideal gas, the spatial distribution of gas-dynamic parameters between the wall and the shock is nonuniform due to the volumetric kinetic energy dissipation (term I in the conservation equations). When granular density falls below the cutoff level or exceeds it, volumetric dissipation starts or stops, respectively [10]. Hence, the volumetric dissipation term vanishes at the packed bed and distributions of density and velocity are uniform.

Some flow features were not reported in the previous work, such as the fluidized region downstream of the shock and the compacted solid-block region adjacent to the wall. The advent results show that pressure oscillates in various frequencies at the packed bed region. Dominant wavelength, measured directly from Fig. 4, is around 2.4 cmin the solid block (densely packed bed) for the first case. The wavelength at the fluidized region (from shock front to the packed bed) is 0.5 cm. The second case has higher frequency and the wavelengths are about 1.8 cm (solid region) and 0.3 cm (fluidized region) since the dissipation term induces more energy losses in this case. Pressure in the fluidized region climbs with higher frequency oscillations compared to the solid block, due to the kinetic energy losses. One can observe the invariable length of the fluidized zone from Fig. 7. In case 2, the length of the fluidized region is 1.6 cm, which is compared well with the analytical result in [5]. Also, the speed of the shock becomes faster following an initial transient, especially in case 2, and will ultimately approach some value [5], since shock speed is independent of e and β at the packed solid bed. The shocks in the cases influenced by gravity become stronger with time whereas the cases without gravity exhibit similar behaviour at various times in the entire fluidized region.

6. Conclusion

A numerical algorithm for the computation of granular layer parameters arising in a granular gas is developed. To implement this technique a Roe-type solution to the Rimmen problem is applied. The proposed algorithm enables to obtain solutions for all stages of the shock wave evolution. The governing equations proposed here assume that volumetric dissipation vanishes when the granular gas volume fraction becomes larger than some cutoff level. In the packed bed region pressure oscillates in various frequencies but a dominant wavelength can be found for each case. Lower frequency oscillations occur in the solid block relative to those in the fluidized region.

Stable and accurate results for a granular gas, colliding with a wall, are obtained by the advent Roe algorithm for hyperbolic equations with non-conservative terms and the MUSCL-Hancock time-integration procedure. The Roe-averaged state derived in [10] will not significantly affect the accuracy of the results presented therein since a shock-fitting technique was employed at a discontinuity where the largest error is expected to occur. But the Roe-averaged state applied now enables any gas-dynamic discontinuity to be captured by construction since the resulting algorithm is consistent with the associated

Rankine–Hugoniot jump relations. Results for nonzero initial velocity case show stability and capability to capture shocks, compared to those given in [16] under the same conditions (shocks captured at time 0.23 in Case 1). In this work, the non-conservative term is incorporated in the numerical flux formula to be consistent with upwind principles associated with the granular speed of sound. A one-dimensional test case was analyzed and demonstrated the validity and accuracy of the advent approach to capture strong shocks with the flow features of a fluidized region downstream of the shock and a compacted solid-block region adjacent to the wall. Finally, non-conservative terms often arise in governing equations encountered in turbulence modelLing and the present work may be of relevance in such applications as well. The future work will be to develop this granular-gas model into multi-dimension. The above Roe-averaged scheme is also interested to be investigated in two-phase transient flow models.

Acknowledgments

Professor Hemant Kamath passed away before this paper was issued. His family and I (his student) wish to publish it in his memory. I wish to thank Dr. Palaniyandi Jawahar, for the very useful discussions and advice on the final version of this work. It was with his unstinted help that the math equations were edited and intermediate steps added in the Appendices A.1 and A.2. I thank Dr. Sampath Palanisamy of Metacomp Technologies for generously offering support, Dr. Uri Goldberg, his colleague, for reviewing the early draft of the paper and putting the grammar in shape. I also thank the reviewers for their useful comments to lead this work to the final version.

Work in this paper was carried out at Mads Clausen Institute, University of Southern Denmark.

Appendix A. Roe-averages for the granular-gas model

The Eq. (19) can be expanded using (21) and (2) with appropriate left and right states:

$$(\hat{\rho}\epsilon\widehat{G}_\rho + \widehat{G}\hat{u}^2/2 - \hat{u}^2)(\rho_R - \rho_L) + (2 - \widehat{G})\hat{u}(\rho_R u_R - \rho_L u_L) + \widehat{G}(E_R - E_L) = (\rho_R u_R^2 - \rho_L u_L^2) + (P_R - P_L) \tag{43}$$

A.1. Consistency check in the absence of G

Dropping the terms containing G from Eq. (43) results in a quadratic equation for velocity $\hat{u}$. It can be shown that the solution of the resulting quadratic equation returns the Roe-average for u.

$$(\rho_R - \rho_L)\hat{u}^2 - 2(\rho_R u_R - \rho_L u_L)\hat{u} + (\rho_R u_R^2 - \rho_L u_L^2) = 0 \tag{44}$$

The solutions to this quadratic equation are:

$$\hat{u} = \frac{2(\rho_R u_R - \rho_L u_L) \pm \sqrt{4(\rho_R u_R - \rho_L u_L)^2 - 4(\rho_R - \rho_L)(\rho_R u_R^2 - \rho_L u_L^2)}}{2(\rho_R - \rho_L)}$$

After expanding the terms inside the square root, canceling the like terms and rewriting the denominator we get:

$$\hat{u} = \frac{(\rho_R u_R - \rho_L u_L) \pm \sqrt{\rho_R}\sqrt{\rho_L}(u_R - u_L)}{(\sqrt{\rho_R}^2 - \sqrt{\rho_L}^2)}$$

This can be rewritten as:

$$\hat{u} = \frac{(\sqrt{\rho_R}\sqrt{\rho_R}u_R - \sqrt{\rho_L}\sqrt{\rho_L}u_L) \pm (\sqrt{\rho_R}\sqrt{\rho_L}u_R - \sqrt{\rho_R}\sqrt{\rho_L}u_L)}{(\sqrt{\rho_R} - \sqrt{\rho_L})(\sqrt{\rho_R} + \sqrt{\rho_L})}$$

Choosing the one that yields positive root and re-grouping the terms:

$$\hat{u} = \frac{\sqrt{\rho_R}\sqrt{\rho_R}u_R - \sqrt{\rho_L}\sqrt{\rho_R}u_R - \sqrt{\rho_L}\sqrt{\rho_L}u_L + \sqrt{\rho_R}\sqrt{\rho_L}u_L}{(\sqrt{\rho_R} - \sqrt{\rho_L})(\sqrt{\rho_R} + \sqrt{\rho_L})}$$

which yields the Roe-average for u

$$\hat{u} = \frac{\sqrt{\rho_R}u_R + \sqrt{\rho_L}u_L}{\sqrt{\rho_R} + \sqrt{\rho_L}}$$

A.2. Derivation of Eq. (25)

Terms containing $\hat{u}$ in Eq. (43) can be rearranged as below:

$$\left[\hat{\rho}\epsilon\widehat{G}_\rho + \left(\frac{\widehat{G}}{2} - 1\right)\hat{u}^2\right](\rho_R - \rho_L) + (2 - \widehat{G})\hat{u}(\rho_R u_R - \rho_L u_L) + \widehat{G}(E_R - E_L) = \left(\rho_R u_R^2 - \rho_L u_L^2\right) + (P_R - P_L) \tag{45}$$

Above expression is rewritten in order to simplify as below:

$$\hat{\rho}\epsilon\widehat{G}_{\rho}(\rho_R-\rho_L)+\Phi=(P_R-P_L) \tag{46}$$

where Φ is given as:

$$\Phi=(2-\widehat{G})\left[\frac{-\hat{u}^2}{2}(\rho_R-\rho_L)+\hat{u}(\rho_R u_R-\rho_L u_L)\right]+\widehat{G}(E_R-E_L)-\left(\rho_R u_R^2-\rho_L u_L^2\right) \tag{47}$$

Using the expression for $\hat{u}$ from Eq. (22) and recognising:

$$(\rho_R-\rho_L)=(\sqrt{\rho_R}-\sqrt{\rho_L})(\sqrt{\rho_R}+\sqrt{\rho_L}) \tag{48}$$

the above expression (47) can be re-written as:

$$\begin{aligned}\Phi=(2-\widehat{G})&\left[\left(\frac{-1}{2}\right)\frac{(u_L\sqrt{\rho_L}+u_R\sqrt{\rho_R})^2}{(\sqrt{\rho_L}+\sqrt{\rho_R})^2}(\sqrt{\rho_R}-\sqrt{\rho_L})(\sqrt{\rho_R}+\sqrt{\rho_L})+\left(\frac{u_L\sqrt{\rho_L}+u_R\sqrt{\rho_R}}{\sqrt{\rho_L}+\sqrt{\rho_R}}\right)(\rho_R u_R-\rho_L u_L)\right]\\&+\widehat{G}(E_R-E_L)-\left(\rho_R u_R^2-\rho_L u_L^2\right)=\frac{(2-\widehat{G})}{2(\sqrt{\rho_L}+\sqrt{\rho_R})}\left[-\left(\rho_L u_L^2+\rho_R u_R^2+2\sqrt{\rho_L}\sqrt{\rho_R}u_L u_R\right)(\sqrt{\rho_R}-\sqrt{\rho_L})\right.\\&\left.+2(u_L\sqrt{\rho_L}+u_R\sqrt{\rho_R})(\rho_R u_R-\rho_L u_L)\right]+\widehat{G}(E_R-E_L)-\left(\rho_R u_R^2-\rho_L u_L^2\right)\end{aligned}$$

Expanding,

$$\begin{aligned}\Phi=&\left(1-\frac{\widehat{G}}{2}\right)\left(\frac{1}{\sqrt{\rho_L}+\sqrt{\rho_R}}\right)\left[-\rho_L\sqrt{\rho_R}u_L^2-\rho_R\sqrt{\rho_R}u_R^2-2\sqrt{\rho_L}\rho_R u_L u_R+\rho_L\sqrt{\rho_L}u_L^2+\rho_R\sqrt{\rho_L}u_R^2+2\sqrt{\rho_R}\rho_L u_L u_R\right.\\&\left.+2\sqrt{\rho_L}\rho_R u_L u_R-2\sqrt{\rho_L}\rho_L u_L^2+2\sqrt{\rho_R}\rho_R u_R^2-2\sqrt{\rho_R}\rho_L u_L u_R\right]+\widehat{G}(E_R-E_L)-\left(\rho_R u_R^2-\rho_L u_L^2\right)\end{aligned}$$

After cancellations, we are left with the following:

$$\Phi=\left(1-\frac{\widehat{G}}{2}\right)\left(\frac{1}{\sqrt{\rho_L}+\sqrt{\rho_R}}\right)\left[(\sqrt{\rho_L}+\sqrt{\rho_R})(\rho_R u_R^2-\rho_L u_L^2)\right]+\widehat{G}(E_R-E_L)-\left(\rho_R u_R^2-\rho_L u_L^2\right) \tag{49}$$

This can further be simplified which results in the following expression:

$$\Phi=\widehat{G}\left[\left(E_R-\frac{1}{2}\rho_R u_R^2\right)-\left(E_L-\frac{1}{2}\rho_L u_L^2\right)\right] \tag{50}$$

Recall $E=\rho\epsilon+\rho u^2/2$ and the equation of state for granular gas (6) this expression (50) becomes:

$$\Phi=\widehat{G}\left(\frac{P_R}{G_R}-\frac{P_L}{G_L}\right) \tag{51}$$

Combining Eqs. (46) and (51) one can obtain Eq. (25):

$$\hat{\rho}\epsilon\widehat{G}_{\rho}(\rho_R-\rho_L)+\widehat{G}\left(\frac{P_R}{G_R}-\frac{P_L}{G_L}\right)=P_R-P_L$$

If $\rho_L=\rho_R$, the following equations can be derived:

$$G_L\equiv G(\rho_L)=G_R\equiv G(\rho_R) \tag{52}$$

Then, the both sides of Eq. (25) are equal. If $\rho_L\neq\rho_R$, G can be solved with prescribed Roe-averages $\rho\epsilon$ and G_ρ. It should be noted that the second Eq. (43), expanded from (19) is consistent with the jump condition.

A.3. Consistency of the jump conditions with the proposed algorithm

The terms, containing $\widehat{G}$ in Eq. (43) are:

$$\left[\widehat{G}_{\rho}\left(\widehat{E}-\frac{\hat{\rho}\hat{u}^2}{2}\right)+\hat{u}^2\frac{\widehat{G}}{2}\right](\rho_R-\rho_L)-\hat{u}\widehat{G}(\rho_R u_R-\rho_L u_L)+\widehat{G}(E_R-E_L)=P_R-P_L \tag{53}$$

The third equation, expanded from (19) can be written as:

$$\begin{aligned}&\left[\widehat{G}_{\rho}\left(\widehat{E}-\frac{\hat{\rho}\hat{u}^2}{2}\right)\hat{u}+\hat{u}^3\frac{\widehat{G}}{2}-\frac{\widehat{E+P}}{\hat{\rho}\hat{u}}\right](\rho_R-\rho_L)+\left[-\hat{u}^2\widehat{G}+\frac{\widehat{E+P}}{\hat{\rho}}\right](\rho_R u_R-\rho_L u_L)+\hat{u}(1+\widehat{G})(E_R-E_L)\\&=(E_R+P_R)u_R-(E_L+P_L)u_L\end{aligned} \tag{54}$$

We multiply Eq. (53) by -$\hat{u}$ and add to the second Eq. (54) and obtain a equation as follows:

$$-\frac{\widehat{(E+P)}}{\hat{\rho}}\hat{u}(\rho_R-\rho_L)+\frac{\widehat{(E+P)}}{\hat{\rho}}(\rho_R u_R-\rho_L u_L)+\hat{u}(E_R-E_L)=-(P_R-P_L)\hat{u}+(E_R+P_R)u_R-(E_L+P_L)u_L \tag{55}$$

Re-arranging Eq. (55):

$$\frac{\widehat{(E+P)}}{\hat{\rho}}[-\hat{u}(\rho_R-\rho_L)+\rho_R u_R-\rho_L u_L]=-(E_R+P_R)\hat{u}+(E_R+P_R)u_R+(E_L+P_L)\hat{u}-(E_L+P_L)u_L \tag{56}$$

Substituting $\hat{u}$ into the above equation:

$$\begin{aligned}&\frac{\widehat{(E+P)}}{\hat{\rho}}[-(\sqrt{\rho_L}u_L+\sqrt{\rho_R}u_R)(\sqrt{\rho_R}-\sqrt{\rho_L})+\rho_R u_R-\rho_L u_L]\\&=(E_R+P_R)\left[-\frac{(\sqrt{\rho_L}u_L+\sqrt{\rho_R}u_R)}{\sqrt{\rho_L}+\sqrt{\rho_R}}+u_R\right]+(E_L+P_L)\left[\frac{(\sqrt{\rho_L}u_L+\sqrt{\rho_R}u_R)}{\sqrt{\rho_L}+\sqrt{\rho_R}}-u_L\right]\end{aligned}$$

and expanding:

$$\begin{aligned}&\frac{\widehat{(E+P)}}{\hat{\rho}}(-\sqrt{\rho_R}\sqrt{\rho_L}u_L-\rho_R u_R+\rho_L u_L+\sqrt{\rho_L}\sqrt{\rho_R}u_R+\rho_R u_R-\rho_L u_L)\\&=\frac{(E_R+P_R)}{\sqrt{\rho_L}+\sqrt{\rho_R}}(-u_L\sqrt{\rho_L}-u_R\sqrt{\rho_R}+u_R\sqrt{\rho_L}+u_R\sqrt{\rho_R})+\frac{(E_L+P_L)}{\sqrt{\rho_L}+\sqrt{\rho_R}}(u_L\sqrt{\rho_L}+u_R\sqrt{\rho_R}-u_L\sqrt{\rho_L}-u_L\sqrt{\rho_R})\end{aligned}$$

Introducing $\hat{\rho}=\sqrt{\rho_L\rho_R}$ and canceling the like terms of the above equation:

$$\widehat{(E+P)}(-u_L+u_R)=\frac{(E_R+P_R)}{\sqrt{\rho_L}+\sqrt{\rho_R}}(-u_L\sqrt{\rho_L}+u_R\sqrt{\rho_L})+\frac{(E_L+P_L)}{\sqrt{\rho_L}+\sqrt{\rho_R}}(u_R\sqrt{\rho_R}-u_L\sqrt{\rho_R}) \tag{57}$$

Re-organizing Eq. (57):

$$\widehat{(E+P)}(u_R-u_L)=(u_R-u_L)\frac{[(E_R+P_R)\sqrt{\rho_L}+(E_L+P_L)\sqrt{\rho_R}]}{\sqrt{\rho_L}+\sqrt{\rho_R}} \tag{58}$$

The Roe-averaged state for $E+P$ is, if $u_R \neq u_L$:

$$\widehat{E+P}=\frac{(E_R+P_R)\sqrt{\rho_L}+(E_L+P_L)\sqrt{\rho_R}}{\sqrt{\rho_L}+\sqrt{\rho_R}} \tag{59}$$

This expression is already multiplied by density, and hence it has the switched weight of ρ for the Roe-average of $E+P$, which is defined as H the total enthalpy per unit volume of the granular gas. The equality of the third Eq. (54) now holds with the Roe-averages for density, velocity and total enthalpy per unit volume. And the first equation, expended from Eq. (19) is identity, which is easy to check. Then we can conclude that (19) is satisfied with the existing algorithm.

Similarly the Eq. (20) gives:

$$\frac{\widehat{\mathcal{P}}}{\hat{\rho}}\hat{u}(\rho_R-\rho_L)-\frac{\widehat{\mathcal{P}}}{\hat{\rho}}(\rho_R u_R-\rho_L u_L)-\frac{1}{2}\left(\frac{\mathcal{P}_L}{\rho_L}u_L+\frac{\mathcal{P}_R}{\rho_R}u_R\right)(\rho_R-\rho_L)+\frac{1}{2}\left(\frac{\mathcal{P}_L}{\rho_L}+\frac{\mathcal{P}_R}{\rho_R}\right)(\rho_R u_R-\rho_L u_L)=0 \tag{60}$$

Roe-average for $\mathcal{P}$ can be obtained by directly solving Eq. (60) with substitution of the Roe-averages for density and velocity from Eq. (24):

$$\frac{\widehat{\mathcal{P}}}{\sqrt{\rho_L\rho_R}}(\sqrt{\rho_L}u_L+\sqrt{\rho_R}u_R)(\sqrt{\rho_R}-\sqrt{\rho_L})-\frac{\widehat{\mathcal{P}}}{\sqrt{\rho_L\rho_R}}(\rho_R u_R-\rho_L u_L)-\frac{1}{2}\left(\frac{\mathcal{P}_L}{\rho_L}u_L+\frac{\mathcal{P}_R}{\rho_R}u_R\right)(\rho_R-\rho_L)+\frac{1}{2}\left(\frac{\mathcal{P}_L}{\rho_L}+\frac{\mathcal{P}_R}{\rho_R}\right)(\rho_R u_R-\rho_L u_L)=0 \tag{61}$$

Expanding the above equation:

$$\begin{aligned}&\frac{\widehat{\mathcal{P}}}{\sqrt{\rho_L\rho_R}}(\sqrt{\rho_L\rho_R}u_L+\rho_R u_R-\rho_L u_L-\sqrt{\rho_R\rho_L}u_R-\rho_R u_R+\rho_L u_L)\\&-\frac{1}{2}\left(\frac{\mathcal{P}_L}{\rho_L}\rho_R u_L+\frac{\mathcal{P}_R}{\rho_R}\rho_R u_R-\frac{\mathcal{P}_L}{\rho_L}\rho_L u_L-\frac{\mathcal{P}_R}{\rho_R}\rho_L u_R-\frac{\mathcal{P}_L}{\rho_L}\rho_R u_R-\frac{\mathcal{P}_R}{\rho_R}\rho_R u_R+\frac{\mathcal{P}_L}{\rho_L}\rho_L u_L+\frac{\mathcal{P}_R}{\rho_R}\rho_L u_L\right)=0\end{aligned}$$

After cancellations, we obtain:

$$\widehat{\mathcal{P}}(u_L-u_R)-\frac{1}{2}\left(\frac{\mathcal{P}_L}{\rho_L}\rho_R u_L-\frac{\mathcal{P}_R}{\rho_R}\rho_L u_R-\frac{\mathcal{P}_L}{\rho_L}\rho_R u_R+\frac{\mathcal{P}_R}{\rho_R}\rho_L u_L\right)=0$$

Re-arranging the above equation, we have:

$$\widehat{\mathcal{P}}(u_L - u_R) = \frac{1}{2}\mathcal{P}_L\frac{\rho_R}{\rho_L}(u_L - u_R) + \frac{1}{2}\mathcal{P}_R\frac{\rho_L}{\rho_R}(u_L - u_R) \tag{62}$$

Then $\widehat{\mathcal{P}}$ is directly solved from Eq. (20) if $u_L \neq u_R$. Hence the fact is established that (20) always holds with the present algorithm.

Now the above Roe-averages ensure the equality of (19) and (20). Finally, the proposed algorithm is consistent with the associated Rankine–Hugoniot jump relations.

Appendix B. Parameters for the energy-dissipation term

The dependence of key parameters upon the inelasticity, e, roughness coefficient, β and dimensionless rotational moment of inertia, k were evaluated by Goldshtein & Shapiro (1995) as follows, with the sum of α_t and α_r being constant and equal to 4/3.

$$\alpha_t = \frac{2}{3}\left(1 + \frac{a}{b + (a^2 + b^2)^{1/2}}\right) \tag{63}$$

where

$$a = (1 - \beta^2)\frac{1 - k}{1 + k} - 1 + e^2, b = 2k\left(\frac{1 + \beta}{1 + k}\right)^2.$$

In the case of a uniform sphere, the ranges of the inelasticity coefficient, e, roughness, β and dimensionless rotational moment of inertia, k are: $0 < e \leqslant 1, -1 \leqslant \beta \leqslant 1$ and $k = 0.4$.

The inelasticity coefficient, e, is imposed with the following restriction to ensure monotonic dependence of the parameters α_t and α_r on the coefficients e and β.

$$e \geqslant \left(\frac{2k}{1 + k} - \beta\frac{1 - k}{1 + k}\right)^{1/2} \tag{64}$$

The other parameters are as follows:

$$C_0 = -\left(\frac{\pi}{2}\right)^{1/2}\alpha_t^{3/2}\left[1 - e^2 + \left(\frac{1 - \beta^2}{1 + k}\right)\left(k + \frac{\alpha_r}{\alpha_t}\right)\right] \tag{65}$$

$$C_1 = \lambda\chi_k/\chi, C_2 = \lambda\chi_c/\chi + N(F) \tag{66}$$

with the following coefficients in the above equations:

$$\lambda = -\left(\frac{\pi\alpha_t}{2}\right)^{1/2}\left[3(1 - e^2) + \left(\frac{1 - \beta^2}{1 + k}\right)\left(3k - 2 + \frac{\alpha_r}{\alpha_t}\right)\right] \tag{67}$$

$$\chi = \left(\frac{\pi\alpha_t}{2}\right)^{1/2}\left(\frac{3}{4}(1 - e^2)\alpha_t(3\alpha_t - \alpha_r) + \left(\frac{1 - \beta^2}{1 + k}\right)\frac{3}{4}[(3k - 3)\alpha_t\alpha_r + \alpha_r^2 - k\alpha_t^2] + 4\frac{\eta}{k}\left[3\eta\alpha_t + \left(1 - \frac{\eta}{k}\right)(2\alpha_t - \alpha_r)\right]\right) \tag{68}$$

$$\chi_c = -\frac{3}{4}\alpha_r\alpha_t[1 - N(F)] + \frac{4\eta\alpha_t}{(1 + e)k}\left[\eta + \left(\frac{\eta}{k} - 1\right)\frac{\alpha_r}{\alpha_t}\right] \tag{69}$$

$$\chi_k = -\frac{3}{4}\alpha_t\alpha_r \tag{70}$$

where

$$N(F) = \frac{3}{2}(1 - e) + \left(\frac{1 - \beta^2}{1 + k}\right)\left(\frac{k + a_r/a_t}{1 + e}\right) \tag{71}$$

and

$$\eta = \left(\frac{1 + \beta}{1 + k}\right)\frac{k}{2}.$$

In the limit case of smooth spheres, $\beta = -1$, there is no kinetic energy exchange between the translational and rotational degrees of freedom. In this particular case of perfectly smooth particles $\alpha_t = 4/3, C_0 = -(\pi/2)^{1/2}\alpha_t^{3/2}(1 - e^2), C_1 = 0$, and $C_2 = 3/2(1 - e)$.

References

[1] A. Bermudez, M.E. Vazquez, Upwind methods for hyperbolic conservation laws with source terms, Comput. Fluids 23 (1994) 1049–1071.
[2] C.S. Campbell, Rapid granular flows, Ann. Rev. Fluid Mech. 22 (1990) 57–92.
[3] A. Goldshtein, M. Shapiro, Mechanics of collisional motion of granular materials: Part 1. General hydrodynamic equations, J. Fluid Mech. 282 (1995) 75–114.
[4] A. Goldshtein, M. Shapiro, L. Moldavsky, M. Fishman, Mechanics of collisional motion of granular materials: Part 2. Wave propagation through vibrofluidized granular layers, J. Fluid Mech. 287 (1995) 349–382.
[5] A. Goldshtein, M. Shapiro, C. Gutfinger, Mechanics of collisional motion of granular materials: Part 3. Self-similar shock wave propagation, J. Fluid Mech. 316 (1996) 29–51.
[6] A. Goldshtein, M. Shapiro, C. Gutfinger, Mechanics of collisional motion of granular materials: Part 4. Expansion wave, J. Fluid Mech. 327 (1996) 117–138.
[7] H.M. Jaeger, S.R. Nagel, R.P. Behringer, Granular solids, liquids and gases, Rev. Mod. Phys. 68 (1996) 1259–1273.
[8] J.T. Jenkins, M.W. Richman, Grad's 13-moment system for dense gas of inelastic spheres, Arch. Ration. Mech. Anal. 87 (1985) 355–377.
[9] J.T. Jenkins, M.W. Richman, Kinetic theory for plane flows of a dense gas of identical, rough, inelastic circular discs, Phys. Fluids 28 (1985) 3485–3494.
[10] V. Kamenetsky, A. Goldshtein, M. Shapiro, D. Degani, Evolution of a shock wave in a granular gas, Phys. Fluids 12 (2000) 3036–3049.
[11] M.S. Liou, B. van Leer, J.S. Shuen, Splitting of inviscid fluxes for real gases, J. Comput. Phys. 87 (1990) 1–24.
[12] C.K.K. Lun, S.B. Savage, D.J. Jeffery, N. Chepurniy, Kinetic theories of granular flow: inelastic particles in Couette flow and slightly inelastic particles in a general flow field, J. Fluid Mech. 140 (1984) 223–256.
[13] C.K.K. Lun, Kinetic theory for granular flow of dense slightly inelastic, slightly rough spheres, J. Fluid Mech. 233 (1991) 539–559.
[14] P.L. Roe, Approximate Riemann solvers, parameter vectors and difference schemes, J. Comput. Phys. 43 (1981) 357–372.
[15] P.L. Roe, Upwind differencing schemes for hyperbolic conservation laws with source terms, in: C. Carasso, P.A. Raviart, D. Serre (Eds.), Proceeding of Conference on Nonlinear Hyperbolic Problems, Lecture Notes in Mathematics, vol. 1270, Springer-Verlag, New York/Berlin, 1986, pp. 41–51.
[16] S. Serna, A. Marquina, Capturing shock waves in inelastic granular gases, J. Comput. Phys. 209 (2005) 787–795.
[17] S. Serna, A. Marquina, Capturing blast waves in granular flow, Comp. & Fluids 36 (2007) 1364–1372.
[18] P.K. Sweby, High resolution schemes using flux limiters for hyperbolic conservation laws, SIAM J. Numer. Anal. 21 (1984) 995–1011.
[19] B. van Leer, On the relation between the upwind-differencing schemes of Godunov, Engquist-Osher and Roe, SIAM J. Sci. Statist. Comput. 5 (1984) 1–20.
[20] R.J. LeVeQue, Finite Volume Methods for Hyperbolic Problems, Cambridge University Press, Cambridge, 2002.
[21] M. Renardy, R.C. Rogers, An Introduction to Partial Differential Equations, Springer, New York, 2000.